Int J Adv Manuf Technol (2018) 94:599–614
DOI 10.1007/s00170-017-0754-7

ORIGINAL ARTICLE

Three-dimensional finite element modeling of drilling CFRP composites using Abaqus/CAE: a review

Gong-Dong Wang[1,2] · **Stephen Kirwa Melly**[1]

Received: 17 October 2016 / Accepted: 26 June 2017 / Published online: 15 August 2017

Abstract The extra-ordinary properties of carbon fiber reinforced polymer (CFRP) composites and its outstanding performance in their structural applications, especially in aerospace industry where high strength to weight ratio is highly desirable, have given them a steadfast attention in the engineering materials research world. Drilling of CFRP materials to facilitate holes for component assembly subjects them to various modes of failure due to their anisotropy and in homogeneity. A requisite means of investigation and analysis is therefore required in order to understand these failure modes. Traditionally, the failure modes have been studied through experiments and more recently numerical simulations. There are dozens of finite element (FE) software available for numerical simulation with Abaqus/CAE being the mostly used for composites analysis. The numerical setup is a complicated process requiring some level of expertise in order to get accurate results which can be validated with experimental results. Upcoming researchers find it difficult, and they end up spending much time preparing for a successful simulation due to scattered information in scientific literature about modeling. This article tries to make work easier for new researchers by doing a review of 3D modeling of drilling CFRP using Abaqus/CAE software. The article features models from highly experienced researchers and their validated results with step-by-step setup guidelines. The objective is to provide a basic guideline to new researchers on the appropriate material properties and damage models for a successful and accurate simulation.

Keywords Abaqus/CAE · 3D modeling · CFRP · Drilling simulation

✉ Stephen Kirwa Melly
kirwamellie@yahoo.com

[1] School of Aerospace Engineering, Shenyang Aerospace University, N0. 37 Daoyi South Avenue Development District, Shenyang 110136, People's Republic of China

[2] Key Laboratory of Liaoning Province for Composite Structural Analysis of Aero craft and Simulation, Shenyang 110136, People's Republic of China

1 Introduction

The phenomenal performance of carbon fiber reinforced polymer composites (CFRP) in their structural applications has made them materials of choice especially in aerospace industry. The main attributes of these materials are their high strength, high stiffness, and low weight which are highly favorable in aerospace applications. As a result of these properties, the demand of CFRP composites extends to other engineering applications including automotive and sporting industries where high strength and low weight take high precedence. Since the introduction of composites as potential materials of choice in aerospace industry a few decades ago, each year since then, there has been continuous increase in its application on aircraft structures. This replacement of conventional materials like aluminum for structural applications of aircraft has resulted to Airbus A350XWB aircraft boasting of about 53% composites on its structural weight [1].

The manufacturing of these materials can be classified as either primary or secondary manufacturing [2]. Near net shape of the CFRP composites is produced via the primary manufacturing processes. To facilitate component assembly, additional machining operations are required [3]. These operations can be termed as secondary manufacturing processes and will include several holes for rivets and bolts. Hole making is therefore an indispensable secondary manufacturing process. There are several techniques to make holes including

conventional and non-conventional methods. So far, the most commonly employed method to make holes is the conventional drilling with a twist drill. Compared to metallic materials, carbon fiber reinforced composites, despite their attractive nature, raise specific problems during machining and drilling in particular [4]. This difficulty in machining of the said composites is attributed to its material characteristics including non-homogeneity, anisotropy, highly abrasive and hard reinforced fibers, and coexistence of hard abrasive fibers with soft matrix [5]. The damages associated with drilling of CFRP composites, primarily due to its characteristics mentioned above, include excessive tool wear which in turn induces such damage phenomena as fiber pull-out, particle fracture, delamination, and de-bonding at the fiber or particle and matrix interface [6]. Of all the problems caused by drilling on the composite, delamination has been considered as the most severe one [7], and it is the reason why up to 60% of the components are rejected during assembling. It is severe in the sense that it causes significant reduction in the fatigue strength of the component thus degrading the long-term performance of the composite [3]. Delamination therefore is a great loss bearing in mind that drilling is the last machining operation on composites.

The last few years have seen researchers working around the clock to curb this kind of damages to composites during machining. This has led to tremendous amount of literature available about the same and can be found on these state-of-the-art reviews [6–8]. The methods that have been used by researchers in studying the drilling of composites have been diverse and can be generally divided into three categories namely experimental studies focusing on micro/macro machinability of composites, simple modeling using conventional cutting mechanics, and numerical simulations [6]. These kind of studies are focused on various drilling parameters contributing to delamination which include fiber orientations, tool geometry, tool type, feed rate, spindle speed, thrust force, and stacking sequences.

Most of damage evaluation during drilling of composites has been done via experimental means. As has been mentioned, tool geometry plays a role in damage during drilling. C.C Tsao [9] did experimental studies using step core drill in order to find the thrust forces involved. His studies concluded that diameter ratio and feed rate have significant influence on the overall performance of the drill and that this kind of drill produces the highest thrust force (which is related to delamination). The most recent work by Nagaraja et al. [10] investigated experimentally the influence of tool type in drilling of carbon fiber reinforced composites. They used high-speed steel (HSS) and solid carbide drills in their work. The scanning electron microscope images from their results showed that the damage caused by HSS is more severe than that caused by solid carbide drills hence recommending the use of the latter drill type for generating quality holes in composites. Numerous amount of literature is also available concerning the effects of drilling parameters including feed rate, spindle speed, and thrust force. Using step core drills as the tools, the following researchers [11, 12] studied the influence of diameter ratio, feed rate, and spindle speed. They found that the said parameters have influence on delamination and the best combination to be: diameter ratio = 0.74 mm/min, feed rate 8 mm/min, and spindle speed = 1200RPM.

Due to the abrasive nature of the fibers, serious tool wear is normally encountered during drilling. Several researchers have done experimental work concerning this issue of tool wear. Xin Wang et al. [13] studied wear of uncoated and diamond-coated tools during drilling of CFRP. They found that diamond coatings significantly reduce the edge rounding wear. The relationship between tool wear and surface quality has been a concern. Ramirez et al. [14] evaluated experimentally the tool wear and surface integrity of drilled holes in CFRP. They found that the main wear mechanism of the tool is by abrasion and has direct relationship with the quality of the hole surface. Several other experimental studies [15–22] have focused on understanding drilling of carbon fiber reinforced composites.

The advances in technology in the recent years have led to the development of computers with high computing capability. Powerful finite element simulation software has also been developed in the last few decades. The combination of these two developments has been great news to scientists and engineers as it has allowed machining processes to be modeled and simulated in an efficient and accurate manner. Process simulations are therefore replacing physical experiments in almost every aspect of research. Unlike experiments which are costly, time-consuming, can be difficult to perform, and involves destructive techniques, process simulations have many advantages including saving on the costs and time, and variables difficult to obtain in experiments can be predicted.

Numerous papers have been published about finite element simulation model of drilling in CFRP. Phadnis et al. [23] did a successful 3D model of drilling in CFRP composite to predict critical thrust forces and torques that trigger damages to the work piece, and they found their results to be in good agreement with experimental results available in literature. Feito et al. [24] developed a complete and a simplified model of drilling in order to predict delamination. The former involves a complete modeling of the process including rotary movement of the drill, penetration of work piece and element deletion, while the latter considers the drill acting like a punch. While reducing computational cost, the simplified model slightly over-estimated delamination. A 3D model of drilling was developed by the authors [25] in order to study the effects of drill geometry on drilling induced delamination. They used a step drill and a twist drill where they concluded that delamination and other work piece defects could be eliminated by suitable selection of step drill geometry. Non-conventional

drilling methods like ultrasonically assisted drilling (UAD) have been explored as a better way of drilling composites. Some authors [26, 27] have modeled successful finite element simulation of this kind of drilling. It is common for researchers these days to validate their experimental works with finite element simulations for instance the authors [2, 3, 28].

Drilling of composites is undoubtedly most complicated process to study with so many variables to consider. This makes designing experimental procedures capable of complete damage prediction very difficult to achieve. This necessitates for models which are capable of simulating the entire damage process from its initiation through evolution to complete composite structure failure [29]. With the development of powerful computers year in year out, the finite element simulation of machining processes continues to increase. The pioneers of these simulation works have done a great job and laid down foundation for future researchers. Several review papers [7, 30, 31] have been published about experimental drilling studies. Modeling review article available [6] deals with machining of composites and more specifically turning and milling. There is no review paper about 3D finite element simulation of drilling; hence, this article is going to be one of its kind. This paper summarizes the appropriate material properties, damage criterion (for both intra-laminar and inter-laminar), work piece, and tool geometry model for a successful simulation. The main objective is to provide a basic guideline for drilling CFRP simulation setup to upcoming researchers.

2 CFRP material modeling

For a FE simulation to be highly accurate and at the same time reliable, it should be able to predict the stress distributions, forces, torque, and the various damage modes in composites precisely. The essential ingredient for this achievement is an accurate definition of material properties. The failure criteria for laminated composites (2D Hashin failure criterion) are available in Abaqus/CAE. Unfortunately, it can only be applied to shell elements and continuum shell elements making it suitable for 2D problem analysis as it cannot take into account through thickness rate-dependent deformations. For this reason, a constitutive material model and a failure criteria suitable for solid elements (3D stress) should be developed. This is achieved by implementing the Hashin 3D failure criteria in a Vectorized User Material (VUMAT) subroutine available in Abaqus/CAE. This section deals with successful materials models that have been used by researchers.

2.1 Constitutive model for undamaged and damaged laminate

Prior to damage, linear elastic material behavior is assumed for the CFRP laminates. Orthotropic elastic material is therefore modeled with the stress strain relationships as shown in Fig. 1. The elastic constants of the undamaged model are defined as shown in Fig. 2.

where E_i is the Young's modulus in i direction, G_{ij} is the shear modulus in $i-j$ plane, and ν_{ij} is the Poisson's ratio for transverse strain in the j direction, when the stress is in the i direction.

Once the damage initiation criterion is satisfied, the degradation of the material stiffness is begins and is defined by Eq. (1) represented by the 6*6 matrix shown in Fig. 3.

$$\sigma = C(d).\varepsilon,\ \ \sigma_{ij} = C_{ij}.\varepsilon_{ij} \tag{1}$$

The non-zero terms of the damaged laminate matrix shown in Fig. 3 are defined as shown in Fig. 4.where

$$d_f = 1-\left(1-d_{ft}\right)\left(1-d_{fc}\right),\quad d_m = 1-(1-d_{mt})(1-d_{mc}), \Gamma = 1/(1-\nu_{12}\nu_{21}-\nu_{23}\nu_{32}-\nu_{13}\nu_{31}-2\nu_{21}\nu_{32}\nu_{13}).$$

where E_i is the Young's modulus in i direction, G_{ij} is the shear modulus in $i-j$ plane, and ν_{ij} is the Poisson's ratio for transverse strain in the j direction, when the stress is in the i direction. The factors S_{mt} and S_{mc} in the definitions of the shear moduli are introduced to control the reduction in shear

Fig. 1 Stress-strain relation for undamaged laminate [32]

$$\begin{bmatrix}\sigma_{11}\\ \sigma_{22}\\ \sigma_{33}\\ \sigma_{12}\\ \sigma_{23}\\ \sigma_{31}\end{bmatrix} = \begin{bmatrix} C_{11}^0 & C_{12}^0 & C_{13}^0 & 0 & 0 & 0\\ C_{12}^0 & C_{22}^0 & C_{23}^0 & 0 & 0 & 0\\ C_{13}^0 & C_{23}^0 & C_{33}^0 & 0 & 0 & 0\\ 0 & 0 & 0 & C_{44}^0 & 0 & 0\\ 0 & 0 & 0 & 0 & C_{55}^0 & 0\\ 0 & 0 & 0 & 0 & 0 & C_{66}^0 \end{bmatrix} \begin{bmatrix}\epsilon_{11}\\ \epsilon_{22}\\ \epsilon_{33}\\ \epsilon_{12}\\ \epsilon_{23}\\ \epsilon_{31}\end{bmatrix}$$

$$C_{11}^0 = E_1(1-\nu_{23}\nu_{32})\Gamma$$
$$C_{22}^0 = E_2(1-\nu_{13}\nu_{31})\Gamma$$
$$C_{33}^0 = E_3(1-\nu_{12}\nu_{21})\Gamma$$
$$C_{12}^0 = E_1(\nu_{21}+\nu_{31}\nu_{23})\Gamma$$
$$C_{23}^0 = E_2(\nu_{32}+\nu_{12}\nu_{31})\Gamma$$
$$C_{13}^0 = E_1(\nu_{31}+\nu_{21}\nu_{32})\Gamma$$
$$C_{44}^0 = G_{12}$$
$$C_{55}^0 = G_{23}$$
$$C_{66}^0 = G_{13}$$
$$\Gamma = 1/(1-\nu_{12}\nu_{21}-\nu_{23}\nu_{32}-\nu_{13}\nu_{31}-2\nu_{21}\nu_{32}\nu_{13})$$

Fig. 2 Elastic constants for undamaged model [32]

$$C_{11} = (1-d_f)E_1(1-\nu_{23}\nu_{32})\Gamma$$
$$C_{22} = (1-d_f)(1-d_m)E_2(1-\nu_{13}\nu_{31})\Gamma$$
$$C_{33} = (1-d_f)(1-d_m)E_3(1-\nu_{12}\nu_{21})\Gamma$$
$$C_{12} = (1-d_f)(1-d_m)E_1(\nu_{21}-\nu_{31}\nu_{23})\Gamma$$
$$C_{23} = (1-d_f)(1-d_m)E_2(\nu_{32}-\nu_{12}\nu_{31})\Gamma$$
$$C_{31} = (1-d_f)(1-d_m)E_1(\nu_{31}-\nu_{21}\nu_{32})\Gamma$$
$$C_{44} = (1-d_f)(1-s_{mt}d_{mt})E_1(1-s_{mc}d_{mc})G_{12}$$
$$C_{55} = (1-d_f)(1-s_{mt}d_{mt})E_1(1-s_{mc}d_{mc})G_{23}$$
$$C_{66} = (1-d_f)(1-s_{mt}d_{mt})E_1(1-s_{mc}d_{mc})G_{13}$$

Fig. 4 Non-zero terms of the damaged laminate [33]

stiffness caused by tensile and compressive failure in the matrix, respectively.

2.2 CFRP mechanical properties

As already mentioned, using 3D solid elements requires the use of Vectorized User Material (VUMAT) subroutine to implement damage criteria. In this case, the material properties of the CFRP model will be entered as mechanical constants under user material in the property module of the Abaqus/CAE software. To create/enter material properties, go to *property module* > *create material* > *general* > *user material*.

The material properties vary depending on the type of the composite. There are two main configurations namely unidirectional (UD) and woven carbon fibers. The former is widely used in practice and in research and therefore has been extensively covered in literature. Properties of composites are directionally dependent which is why orthotropic material specifications are used in FE analysis. The most commonly used material type in literature is (UD) CFRP T700-M21 and T300/LMT45-EL (UD) as reported by authors [23, 26–28] and [3, 24], respectively. The most prolific authors as far as finite element modeling of drilling in CFRP are Phadnis et al. In all their papers, the authors have used consistent values of composite material properties. Table 1 lists several authors and the orthotropic properties of CFRP composites they used in their studies.

$$\begin{bmatrix}\sigma_{11}\\ \sigma_{22}\\ \sigma_{33}\\ \sigma_{12}\\ \sigma_{23}\\ \sigma_{13}\end{bmatrix} = \begin{bmatrix} C_{11}^0 & C_{12}^0 & C_{13}^0 & & & \\ C_{12}^0 & C_{22}^0 & C_{23}^0 & & & \\ C_{13}^0 & C_{23}^0 & C_{33}^0 & & & \\ & & & C_{44}^0 & & \\ & & & & C_{55}^0 & \\ & & & & & C_{66}^0 \end{bmatrix} \begin{bmatrix}\varepsilon_{11}\\ \varepsilon_{22}\\ \varepsilon_{33}\\ \varepsilon_{12}\\ \varepsilon_{23}\\ \varepsilon_{13}\end{bmatrix}$$

Fig. 3 Stress-strain relations for damaged laminate [33]

2.3 CFRP damage

CFRP composites consist of two parts, the matrix, and the reinforcement. The reinforcements in this case are carbon fibers which are meant to provide strength. The purpose of the matrix is to bind the reinforcements together and can be a polymer resin such as epoxy. This therefore leads to two different failure modes; matrix failure and fiber failure commonly referred to as intra-laminar failure. The most severe form of damage is delamination also known as inter-laminar failure.

2.3.1 Intra-laminar damage

Intra-laminar damage consists of matrix and fiber damage as already mentioned. There are several theories that explain this kind of failure. These include Hashin, Hou, Tsai-wu, and Tsai-Hill. Hashin criterion [37] is the most commonly used failure criterion for analysis of composites using Abaqus/CAE. Despite being used extensively, some studies [6] have found that Hashin's criterion cannot accurately predict the initiation of matrix damage. This has led to researchers using other alternative criteria for analysis.

Table 1 Mechanical properties of CFRP

Author	CFRP orthotropic properties
1. V.A Phadnis et al. [3, 26, 28]	$E_{11}=127GPa,\ E_{22}=E_{33}=9.1GPa,\ \upsilon_{12}=\upsilon_{13}=0.31,\ \upsilon_{23}=0.45,\ G_{12}=G_{13}=5.6GPa,\ G_{23}=4GPa,\ \rho=1600kg/m^3$
2. O. Isbilir and E. Ghassemieh [25]	$E_{11}=112GPa,\ E_{22}=E_{33}=8.2GPa,\ G_{12}=G_{13}=4.5GPa\ G_{23}=3GPa, \upsilon_{12}=\upsilon_{13}=0.3, \upsilon_{23}=0.4$
3. F. Makhdum et al. [27]	$E_{11}=115GPa,\ E_{22}=E_{33}=14GPa,\ \upsilon_{12}=\upsilon_{13}=0.29,\ \upsilon_{23}=0.4\ G_{12}=G_{13}=4GPa, G_{23}=3.2GPa$
4. Y. Shi et al. [34]	$E_{11}=153GPa,\ E_{22}=E_{33}=10.3GPa,\ \upsilon_{12}=\upsilon_{13}=0.3,\ \upsilon_{23}=0.4,\ G_{12}=G_{13}=6GPa, G_{23}=3.7GPa,$
5. H. Singh and P. Mahajan [35]	$E_{11}=143.4GPa,\ E_{22}=E_{33}=9.27GPa,\ G_{12}=G_{13}=3.8GPa,\ G_{23}=3.2GPa,\ \upsilon_{12}=\upsilon_{13}=0.31,\ \upsilon_{23}=0.52,\ \rho=1600kg/m^3$
6. L. Raimondo et al. [36]	$E_{11}=114GPa,\ E_{22}=E_{33}=8.6GPa,\ \upsilon_{12}=\upsilon_{13}=0.3,\ \upsilon_{23}=0.46,\ G_{12}=G_{13}=4.45GPa, G_{23}=4GPa$

i. Hashin criteria

The most extensively used criteria in the industry. It is also included in the finite element code Abaqus/CAE. It was postulated by Zvi Hashin, a mechanical engineer and a retired professor of solid mechanics at Tel-Aviv University, in 1980. Hashin's criterion considers four different modes of failure for a composites namely fiber tension, fiber compression, matrix tension, and matrix compression as expressed by Eqs. (2)–(5).

Fiber tension $\sigma_{11}\geq 0$

$$\left(\frac{\sigma_{11}}{X_T}\right)^2+\frac{\sigma_{12}^2+\sigma_{13}^2}{S_{12}^2}=\begin{cases}\geq 1 & failure\\ <1 & \text{no } failure\end{cases} \tag{2}$$

Fiber compression $\sigma_{11}<0$

$$\left(\frac{\sigma_{11}}{X_C}\right)^2=\begin{cases}\geq 1 & failure\\ <1 & \text{no } failure\end{cases} \tag{3}$$

Matrix tension $\sigma_{22}+\sigma_{33}>0$

$$\frac{(\sigma_{22}+\sigma_{33})^2}{Y_T^2}+\frac{\sigma_{23}^2-\sigma_{22}\sigma_{33}}{S_{23}^2}+\frac{\sigma_{12}^2+\sigma_{13}^2}{S_{12}^2}=\begin{cases}\geq 1 & failure\\ <1 & \text{no } failure\end{cases} \tag{4}$$

Matrix compression $\sigma_{22}+\sigma_{33}<0$

$$\left[\left(\frac{Y_C}{2S_{23}}\right)^2-1\right]\left(\frac{\sigma_{22}+\sigma_{33}}{Y_C}\right)+\frac{(\sigma_{22}+\sigma_{33})^2}{4S_{23}^2}+\frac{\sigma_{23}^2-\sigma_{22}\sigma_{33}}{S_{23}^2}+\frac{\sigma_{12}^2+\sigma_{13}^2}{S_{12}^2}=\begin{cases}\geq 1 & failure\\ <1 & \text{no } failure\end{cases} \tag{5}$$

where σ_{ij} is the stress components, subscripts T and C are the tensile and compressive strengths of the laminate, X_T and Y_T are the allowable tensile strengths, X_C and Y_C are the allowable compressive strengths, and S_{12}, S_{13}, andS_{23} are the allowable shear strengths.

The input values for Hashin's criterion damage parameters have been recorded by various researchers and are listed in Table 2.

ii. Hou criteria

Several authors including [24, 39–41] have used Hou criteria to model intra-laminar failure in their research and hence have been used widely in literature. It considers three different types of damage in intra-laminar failure and also considers delamination (inter-laminar failure). So, the unique part of this criteria is

Table 2 Hashin's damage parameters

Author	Hashin damage parameters
1. V.A. Phadnis et al. [3]	$X_T=2720MPa,\ Y_T=111MPa,\ X_C=1690MPa,\ S_{12}=115MPa,\ S_{23}=40MPa$
2. O. Isbilir and E. Ghassemieh [25, 38]	$X_T=1900MPa, Y_T=84MPa,\ X_C=1000MPa,\ Y_C=250MPa,\ S_{12}=60MPa,\ S_{23}=110MPa$
3. Y. Shi et al. [34]	$X_T=2537MPa,\ X_C=1580MPa,\ Y_T=82MPa,\ Y_C=236MPa,\ S_{12}=90MPa,\ S_{23}=40MPa$

that it also models delamination which the Hashin criteria does not. The three different types of damage (fiber failure, matrix cracking, and matrix crushing) are shown in Eqs. (6)–(8), whereas delamination damage is shown in Eq. (9).

Fiber failure

$$d_f^t = \left(\frac{\sigma_{11}}{X_t}\right)^2 + \left(\frac{\tau_{12}}{S_{12}}\right) \leq 1 \tag{6}$$

Matrix cracking

$$d_m^t = \left(\frac{\sigma_{22}}{Y_t}\right)^2 + \left(\frac{\tau_{12}}{S_{12}}\right)^2 \leq 1 \tag{7}$$

Matrix crushing

$$d_m^c = \frac{1}{4}\left(\frac{-\sigma_{22}}{S_{12}}\right)^2 + \left(\frac{Y_c^2\sigma_{22}}{4S_{12}^2 Y_c}\right)^2 - \left(\frac{\sigma_{22}}{Y_c}\right) + \left(\frac{\tau_{12}}{S_{12}}\right)^2 \leq 1 \tag{8}$$

Delamination

$$d_{del}^2 = \left(\frac{\sigma_{33}}{t_n}\right)^2 + \left(\frac{\sigma_{13}}{t_s}\right)^2 + \left(\frac{\sigma_{23}}{t_t}\right)^2 \geq 1 \tag{9}$$

In the above equations, σ_{11} , σ_{22}, and σ_{12} are stress components in fiber, transverse direction, and in-plane shear stress, respectively. X_t, Y_t, Y_c, and S_{12} are tensile strength in transverse direction, tensile strength in longitudinal direction, transverse compressive strength, and in-plane shear strength, respectively.

The values for the above parameters as have been reported by authors [24] are listed in Table 3.

iii. Puck's criteria

As already mentioned, Hashin criteria has been reported not to predict matrix compression failure accurately. An alternative failure model suggested by Puck and Schurmann [42] has been widely accepted as a better way of predicting matrix failure. Several authors including [3, 23] used this criterion to model matrix failure whereas using Hashin criterion for fiber damage. Equation (10) shows Puck's criteria for matrix failure.

Table 3 Hou criteria parameters

Property	Value
X_t(MPa)	2720
X_c(MPa)	1690
Y_c (MPa)	240
S_{12}(MPa)	115
$t_s = t_t$ (MPa)	90
t_n (MPa)	60

$$\left[\left(\frac{\sigma_{11}}{2X_{1t}}\right)^2 + \frac{\sigma_{22}^2}{|X_{2t}.X_{2c}|} + \left(\frac{\sigma_{12}}{S_{12}}\right)^2\right] + \sigma_{22}\left(\frac{1}{X_{2t}} + \frac{1}{X_{2c}}\right) = 1 \tag{10}$$

where σ_{11} , σ_{22}, and σ_{12} are the stress components, andX_{1t}, X_{2t}, and X_{2c} are the tensile failure stress in fiber direction, transverse direction, and compressive failure stress in transverse direction, respectively. S_{12} is shear failure stress in 2–3 plane.

2.3.2 Inter-laminar damage

Inter-laminar damage is defined in the interaction module of the Abaqus/CAE software. In the *interaction module* > *create interaction property* > *contact* > *mechanical*; tangential, normal, cohesive, and damage parameters are entered. There are two approaches that have been employed by researchers to model inter-laminar damage, otherwise known as delamination. In most of the studies, this is the main focus or the main subject of study as far as CFRP composites are concerned. It is considered as the most severe form of damage because it affects the structural integrity and long-term reliability of the composite components [38]. The two approaches used are surface-based cohesive behavior and cohesive zone elements. The former is a bit easy to implement, whereas the latter needs expertise.

i. Surface-based cohesive behavior

In this approach, the delamination initiation and propagation are modeled as a surface-based interaction property which is available in Abaqus/CAE. It defines cohesive behavior between two adjacent plies one of them as a master and the other as a slave. Several authors including [25, 35, 38] have used this kind of model. It has overall advantages over the surface-based cohesive elements as it is easier to use and reduces the computational cost significantly. Linear elastic response up to delamination is ensured by traction-separation law and then followed by linear softening phase as delamination grows.

Normal stresses σ_n and shear stresses (σ_s, σ_t) are defined for surface-based behavior using the following governing Eqs. (11) as explained by the authors [38].

$$\sigma_i = \begin{cases} k_i\delta_i & D < 1 \\ k_i\delta_i(1-d) & D \geq 1 \end{cases} \cdot i = n, s, t \tag{11}$$

where k is the traction-separation stiffness modulus, δ is the separation for normal and shear directions, and D is the damage variable.

Once the damage is initiated, the specification of its

evolution can be done by using a softening criterion as shown in Eq. (12) where d is the damage variable, whereas δ_m is the effective displacement.

$$d = \frac{\delta_m^f\left(\delta_m - \delta_m^0\right)}{\delta_m\left(\delta_m^f - \delta_m^0\right)} \tag{12}$$

where δ_m is defined as shown in Eq. (13) below.

$$\delta_m = \sqrt{\sum_{i=n}^{i=t} \delta_i^2}. \quad i = n, s, t \tag{13}$$

Total fracture energy at the completion of the delamination is the sum total of normal, tangential, and fracture energies based on power law energy criterion as shown in Eq. (14).

$$\Delta = \left\{\frac{G_n}{G_n^C}\right\}^{\alpha} + \left\{\frac{G_s}{G_s^C}\right\}^{\beta} + \left\{\frac{G_t}{G_t^C}\right\}^{\gamma} \tag{14}$$

where α, β, and γ are exponential constants, whereas G_n^C, G_s^C, and G_t^C are critical fracture energies. Values of these cohesive surface parameters that have been used in literature [25, 34, 38] are given in Table 4.

ii. Cohesive zone elements

This delamination failure model has been used extensively by Phadnis et al. [23, 26, 28] in their several studies about CFRP. Other authors [3, 24, 34] have also used the same to model delamination failure in composites. In this case, cohesive elements available in Abaqus/CAE of a given thickness (mostly 5 μm) are introduced into the layer interfaces. Interface properties are then assigned to these elements. Turon et al. [43] suggested an empirical formula to calculate elastic stiffness that characterizes pre-damage response of cohesive elements. The authors Phadnis et al. employed this formula in their several studies. The formula is shown in Eq. (15) below.

Table 4 Cohesive surface parameters

Parameter	Value
σ_n(MPa)	60
σ_t (MPa)	110
σ_s(MPa)	110
G_n^C (N/mm)	0.33
G_t^C (N/mm)	1.209
G_s^C (N/mm)	1.209

$$K = \frac{\alpha E_{33}}{t} \tag{15}$$

where K, E_{33}, t, and α are interface stiffness, Young's modulus of CFRP laminate in the thickness direction, thickness of the individual ply, and adjusting parameter, respectively. The adjusting parameter is such that for its value greater than 50, the loss of stiffness due to presence of interface is less than 2% [3]. The damage initiation of the cohesive elements has the condition shown in Eq. (16) below.

$$\left[\frac{t_n}{t_n^0}\right]^2 + \left[\frac{t_s}{t_s^0}\right]^2 + \left[\frac{t_t}{t_t^0}\right]^2 = 1 \tag{16}$$

where t_n, t_s, and t_t are the instantaneous components of normal and shear tractions, whereas t_n^0, t_s^0, and t_t^0 represent the peak values of nominal stress. Bilinear traction-separation response as shown in Fig. 5 is used to model the mixed-mode damage of cohesive elements.

When the damage initiation condition is fulfilled, delamination starts and stiffness begins to degrade linearly linked to damage variable d as shown in Eq. (12), the same case as for cohesive surface behavior. The material parameters to model interface cohesive elements are shown in Table 5.

2.3.3 Comparisons of cohesive surface behavior and cohesive zone elements

While both approaches model adhesive surfaces, there exist slight differences between the two. The formulas and laws that govern surface-based cohesive behavior are very similar to those used for cohesive elements. The differences are listed below.

1. Damage in surface-based behavior is an interaction property, whereas damage in cohesive elements is a material property.
2. For surface-based cohesive behavior, the damage evolution is the degradation of the cohesive stiffness, whereas the damage evolution for cohesive elements describes the degradation of material stiffness.
3. For cohesive elements, the material definition includes mass, whereas cohesive surfaces do not add mass.
4. Cohesive elements are recommended for a more detailed adhesive connection modeling, while cohesive surfaces provide a quick and easy way to model adhesive connections.
5. Additional pre-processing effort and increasing computational cost are experienced in cohesive elements compared to cohesive surfaces.

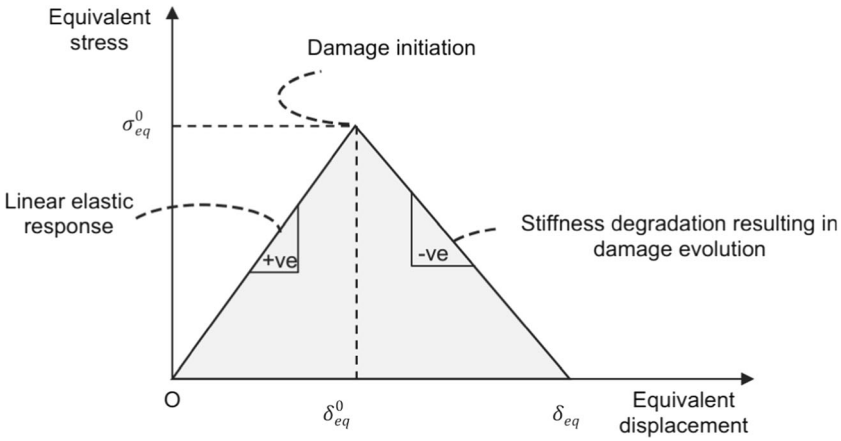

Fig. 5 Damage initiation and evolution in cohesive elements for mode-1 [3]

2.4 Implementation of the failure criterion

In order to use VUMAT subroutine, the Abaqus/CAE software has to be linked with Intel Fortran composer and Microsoft Visual studio all together. Different versions of the software are compatible, and so, the author should have a prior knowledge of compatibility before linking. The VUMAT code is written in Fortran language and linked for analysis in the job module of the Abaqus/CAE (create job > general > user subroutine file). Figure 6 shows algorithm used by authors [3] to implement the failure criterion in Abaqus/Explicit.

3 3D finite Elem Ent part modeling

3.1 Introduction to Abaqus/CAE

Abaqus/CAE (**C**omplete **A**baqus **E**nvironment) is a software suite for finite element analysis and computer-aided engineering. It provides a simple and consistent interface for creating, submitting, monitoring, and evaluating results from Abaqus/Standard and Abaqus/Explicit simulations [44]. Abaqus/CAE is divided into modules where each module defines a logical aspect of the modeling process, for example defining geometry, material properties, assembling, and meshing.

Unlike most of other FE software packages where the user has freedom to choose a system of units to use in the modeling, this cannot be done in Abaqus/CAE as it does not have an inbuilt system of units. The user has to specify all the input data in consistent units. Some commonly used system of units is shown in Table 6.

Table 5 Interface cohesive elements material parameters

Parameter	Value
t_n^0 (MPa)	60
$t_s^0 = t_0^t$ (MPa)	90
G_n(N/mm)	0.2
$G_s = G_t$(N/mm)	1
K_n(N/mm^2)	4×10^6
$K_s = K_t$(N/mm^2)	1×10^6

3.2 Modeling process

The steps involved in a complete setup of a FE model in Abaqus/CAE are represented as a process flow in Fig. 7.

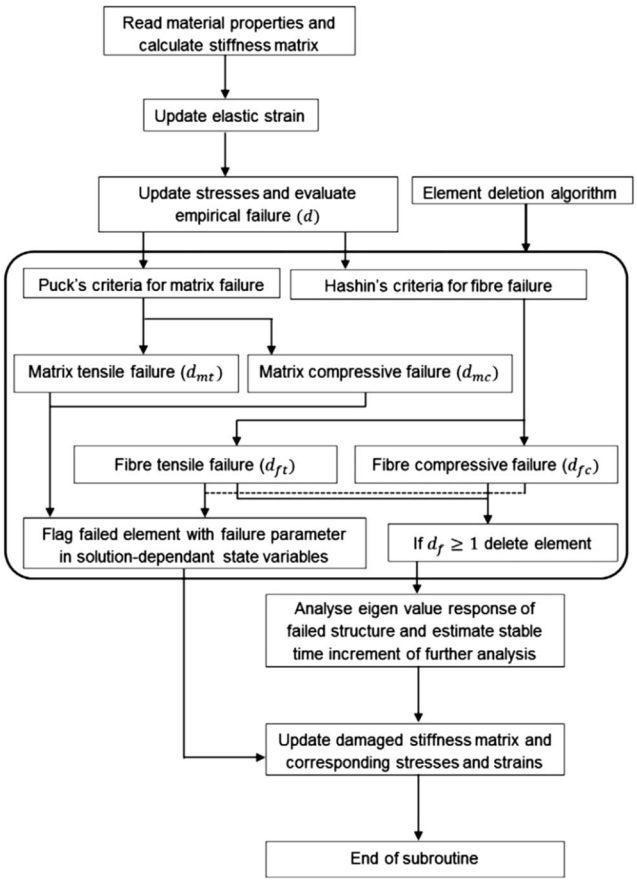

Fig. 6 Algorithm showing implementation of VUMAT [3]

Table 6 Abaqus/CAE consistent units

System of units	Input						Output		
	Length	Force	Elastic modulus	Mass	Density	Gravity (g)	Displacement	Force	Stress
SI	m	N	Pa	kg	kg/m^3	9.807 m/s^2	m	N	Pa
SI (mm)	mm	N	MPa	t (Mg)	t/mm^3	9807 mm/s^2	mm	N	MPa
US unit (ft)	ft	lbf	psf	slug	$slug/ft^3$	32.17 ft/s^2	ft	lb	psf
US units (in)	in	lbf	psi	lbf s^2/in	lbf s^2/in^4	386.1 in/s^2	in	lbf	psi

3.2.1 Part modeling

Modeling is done on the part module of Abaqus/CAE. The module is equipped with all the necessary operations for a complex geometry including 3D, 2D, Axisymmetric, Solid, Shell, Wire, Extrusion, Revolution, and sweep. It is also possible to import parts, assembly, or models of IGS, STEP, Para solid, VDA, or CATIA formats. The dimensions of the geometry depend on the author. It is always recommended to reduce the size of the model as much as possible since big models will mean huge computation work for the computer therefore taking much time to compete the simulation. The number of composite plates to be modeled depends on the number of orientations the author wants to use in the simulation.

The CFRP plate and the drilling tool are modeled as *3D*, *Deformable*, *Solid*, and *Extrusion*. Most of the published work has had the tool being modeled by other 3D modeling software like Computer-Aided Three-Dimensional Interactive Application (CATIA) and then imported to the Abaqus/CAE.

3.2.2 Property assignments

The property module allows the user to create material, create section, assign section, and assign the material orientation. The material properties for the CFRP are entered as mechanical constants under user material since VUMAT subroutine will be used to implement 3D failure criteria. Both the tool and the composite plate have solid and homogenous sections which should be assigned in this module. Finally, material orientation is assigned depending on the stacking sequence the author wants to use in the simulation. The mostly commonly used material orientations are (0° ,45°, −45°, 90°).

3.2.3 Assembling

The author creates instances of the parts in this module and manipulates them according to the experimental setup. The parts can be rotated, translated, or patterned. Figure 8 shows assembled models.

3.2.4 Meshing

In this module, we generate meshes on parts and assemblies created within Abaqus/CAE. Various methods of mesh control are available for the author to create a mesh that meets their analysis. There are three types of mesh formulation available in Abaqus/CAE: Eulerian, Lagrangian, and Arbitrary Lagrangian Eulerian (ALE) [6]. In the Eulerian method, the mesh is spatially fixed, whereas the material is allowed to flow through the meshed control volume thus not suitable for machining simulations. The Lagrangian method is the most suitable for machining simulations since the mesh is attached to material and allowed to deform similarly to actual machining. The main disadvantage of this kind of meshing is severe element distortion and the constant need for

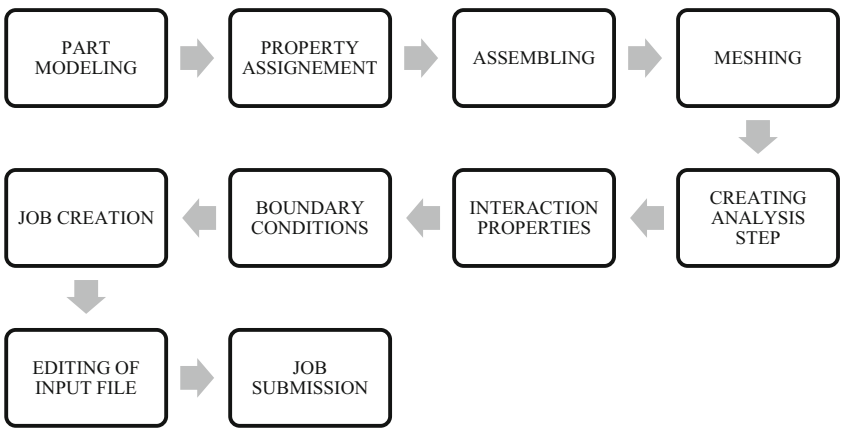

Fig. 7 FE modeling process flow

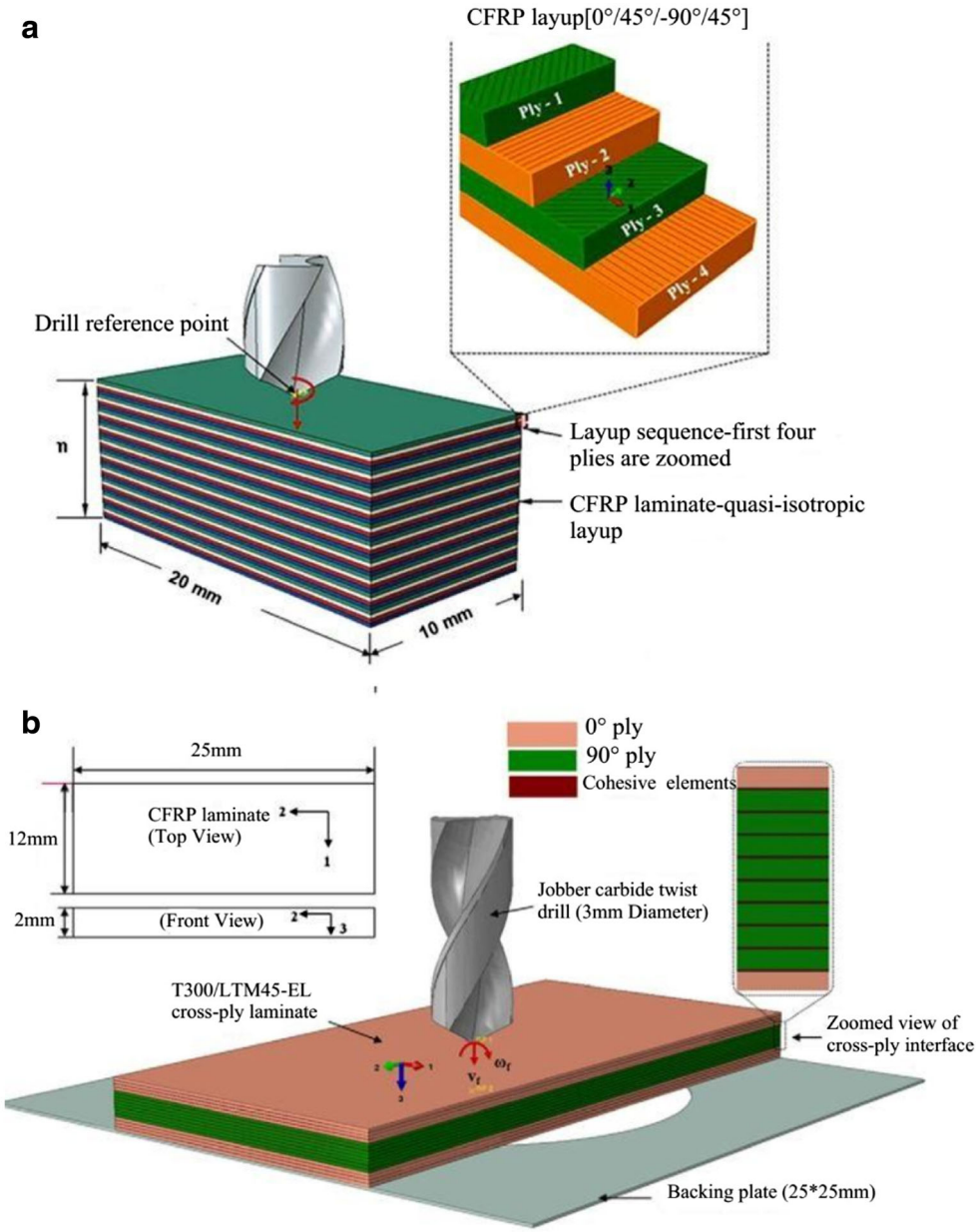

Fig. 8 Assembled models of CFRP drilling. From **a** [27] and **b** [3]

remeshing hence high computation cost. ALE combines Lagrangian and Eulerian formulations hence having advantages of both. It avoids severe distortion without the need for remeshing.

The most popularly used elements for CFRP plate are Reduced-Integrated 8-node brick elements (C3D8R). To simulate delamination, cohesive zone elements, COH3D8 type elements were used. To reduce computational cost as much as possible, the density of mesh around the drilled hole is normally increased to about an aspect ratio of 1, while that of outside the region is reduced. Convergence of the solution is partly determined by the element size. Most researchers will do a convergence study and thus come with a compromise between the element size and the convergence without affecting accuracy of the solution.

The same element type used for the composite plate is also used for the drilling tool. The difference is that the tool elements will be made rigid by using a reference point. A rigid body is a group of elements with the displacement governed by a single node that is the reference point/node. The relative positions of the nodes and elements that are part of the rigid body remain constant throughout a simulation therefore not deforming. Figure 9 shows the meshed assembly.

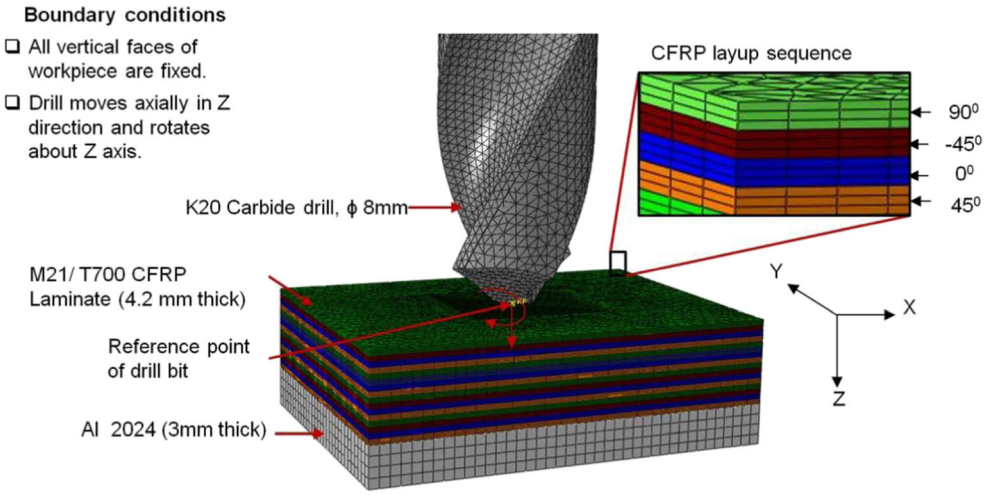

Fig. 9 Meshed Abaqus/CAE model of drilling [23]

3.2.5 Creating analysis step

This module creates analysis steps and specifies the output requests. The initial step is created by default where boundary conditions, predefined fields, and interactions that are applicable at the very beginning of the analysis are defined. The initial step is followed by one or more analysis steps associated with specific procedure that defines the type of analysis to be performed during the step, such as a static stress analysis or a transient heat transfer analysis. For dynamic systems and large non-linear problems like drilling, dynamic explicit time step solves efficiently and therefore is chosen. The time period is chosen depending on the amount of time (determined by feed rate in this case) it will take the tool to complete the drilling process.

3.2.6 Interaction properties

Interaction properties determine how the tool, the work piece, and layers are going to interact during the drilling process. There are two types of interaction properties that are defined. One is for the contact between the tool and the work piece, whereas the other is between the layers of the composite laminate. Normally, the interaction of the tool to the workpiece is of penalty type where friction coefficient is defined. Cohesive surface behavior is defined between each pair of adjacent layers of the laminates. It is also in this cohesive behavior where the damage (delamination) parameters are input including initiation, evolution, and stabilization.

3.2.7 Boundary conditions

The boundary conditions applied should simulate the experimental conditions. Since the drilling tool is modeled as a rigid body, all the boundary conditions to it are assigned to the reference point. The feed rate and the spindle speed are applied to this point using velocity boundary condition. In most cases, the drill is constrained in X and Y directions such that displacements and rotations in this directions are zero (UX = UY = URX = URY = 0). The drill rotation and feed are then applied to the z direction. As for the CFRP composite plate, all the four vertical edges are fixed (UX = UY = UX = URX = URY = URZ = 0) in order to simulate clamping. Figure 10 shows and boundary conditions applied on a composite drilling setup.

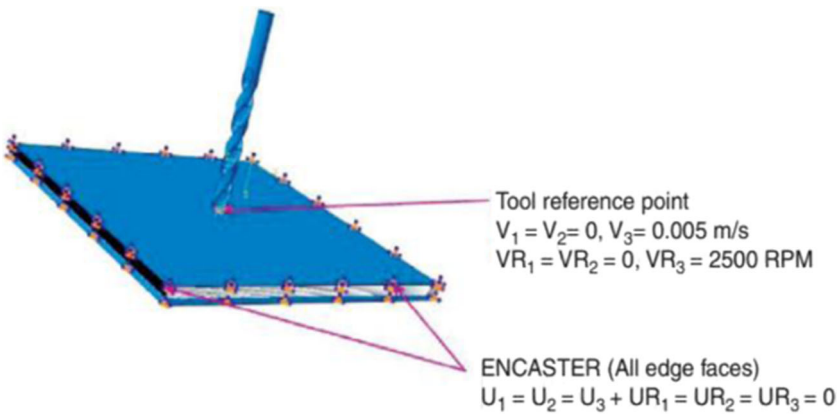

Fig. 10 Boundary conditions [45]

3.2.8 Job creation and editing the input file

The job module allows the user to create job from the model or an input file. By default, the job is created basing on the model. Once the job has been created, the author can write input file on the job manager. The current Abaqus/CAE versions allow interactions only defined using surfaces or nodes. This is disadvantageous, as for 3D drilling, the tool must come in contact with the internal elements of the composite plate. Therefore, editing of the input file is necessary to achieve this kind of interaction.

3.2.9 Job submission

Finally, the job is created again, and this time, the source is chosen as "input file" where the just edited input file is selected. The job is then submitted for calculation and can be monitored for progress.

4 Model validation

In order to have confidence in the finite element model results, comparison with experimental results is necessary. A good agreement between the two is a good news to researchers as it means the finite element model can be used to predict drilling of CFRP under a wide range of drilling parameters very difficult to achieve in experiments. The areas of interest include thrust forces, delamination, and torques. Previous research work has proved that thrust force is directly proportional to the delamination and that is why keeping a keen eye on it is really important.

4.1 Thrust forces

One of the key indicators to describe the quality of drilled holes is thrust force. This is because research has shown that it is directly responsible for drilling induced delamination hence affecting quality of the holes. The authors [46, 47] reported that drilling induced delamination, especially the push-down delamination, correlates closely with the thrust force. In their studies, they found that delamination at the hole exit is directly linked to the drilling thrust force and is believed that there is a "critical thrust force" below which no damage occurs.

Various analytical models have been developed to predict the critical thrust force beyond which delamination initiates. The first ever and the most accepted and referred model is that of Hocheng and Dharan [21] as shown in equation below.

$$F_{crit} = \pi \left[\frac{8 G_{Ic} E_1 h^3}{3\left(1-\upsilon_{12}^2\right)} \right]^{1/2} \tag{17}$$

where F_{crit} is the critical thrust force, E_1 is the elastic modulus, υ_{12} is the Poisson ratio, G_{Ic} is the inter-laminar fracture toughness in mode 1, and h is the uncut plate thickness.

In the FE simulation model, thrust force is recorded by a reference point on the drilling tool. First, a set of the reference point is created, and then on the history output, the domain is selected as "set" where the name of the point is selected and then the output variables to be chosen are the thrust forces.

The authors Phadnis et al. [3] did an excellent job involving both experiments and finite element model to study drilling in carbon/epoxy composites. Their FE model predicted very accurately both the forces, torques, and delamination, as their comparison with experimental results had very little deviations. Several factors that could improve the accuracy of the FE results as reported by the authors include the use of a more realistic friction model, inclusion of thermal effects, and accounting for drill wear effects. Figure 11i–iii shows the comparisons of experimental and finite element results of thrust forces and torques done by various researchers. The comparisons show a very good agreement with reasonable deviations.

4.2 Delamination

The drilling induced delamination has been considered as the most severe form of damage [3] to the composite components as it reduces the structural strength. Delamination damage occurs both at the drilling tool entrance as well as at the tool exit commonly known as peel up and push down delamination, respectively [5], as illustrated in Fig. 12.

Peel-up delamination is caused by the cutting force pushing the cut materials to the flute surface, whereas push-down delamination is caused by thrust force bending the residual laminates just before exit. The most common method of assessing the level of delamination damage is the one-dimensional delamination factor (F_d) which can be defined as the ratio of maximum diameter ($D_{\max}$) of the observed delamination zone to the nominal diameter (D_{nom}) as shown in Eq. 18.

$$F_d = \frac{D_{\max}}{D} \tag{18}$$

Figure 13 illustrates how to measure the maximum and nominal diameters in a drilled hole. Some authors [51] have suggested that the use of F_d may not truly reveal delamination, as a few peeled up or pushed down layers do not represent the true delamination zone of the drilled piece. They suggested a two-dimensional delamination factor F_a as shown in Eq. 19 where A_{nom} *and* A_{del} are nominal and delaminated areas as shown in Fig. 13.

$$F_a = \left(\frac{A_{del} - A_{nom}}{A_{nom}} \right) \% \tag{19}$$

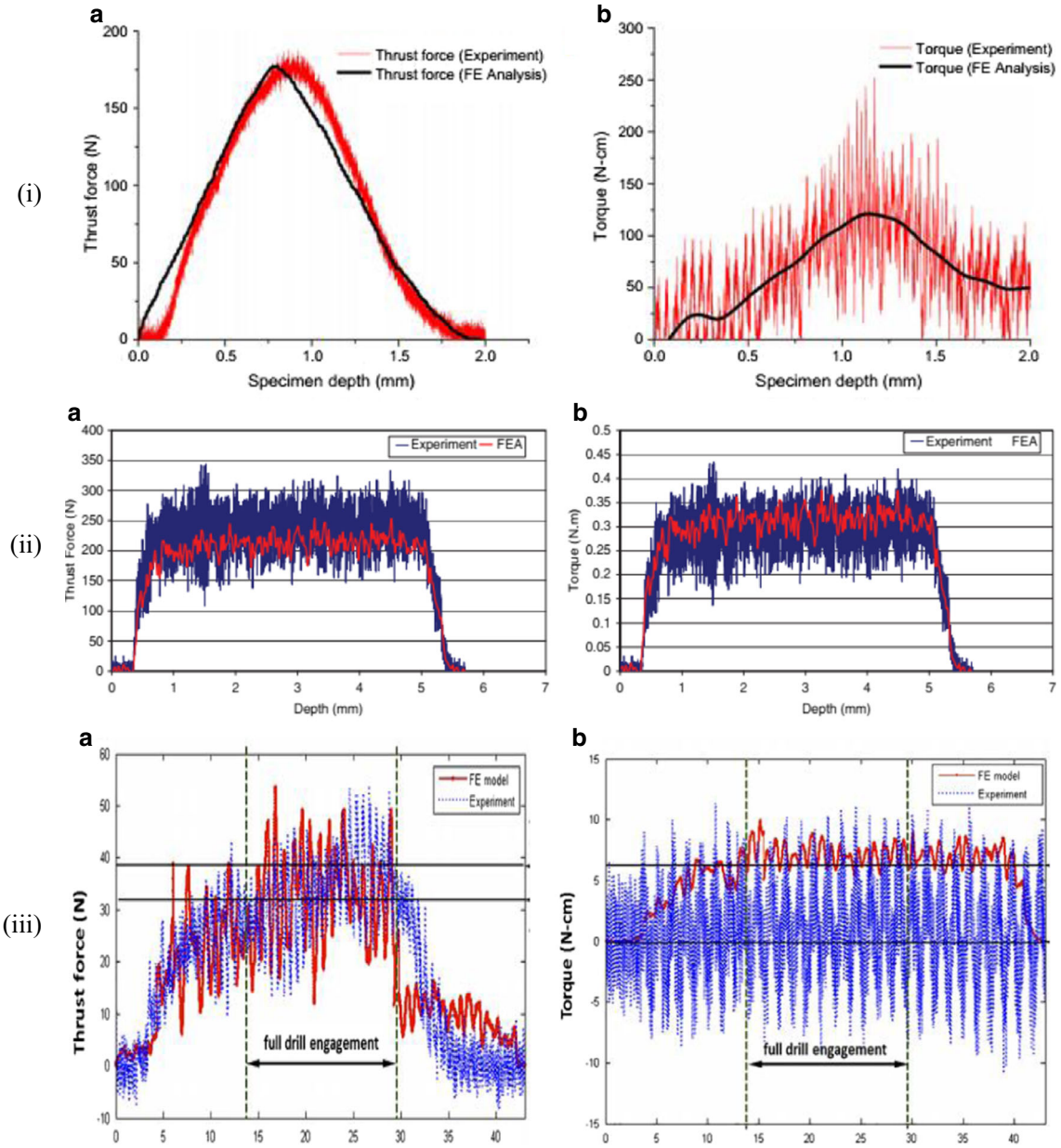

Fig. 11 From **i** [3], **ii** [38], and **iii** [27]. Comparisons of FE and experimental results (**i**–**iii**): thrust forces (*a*) and torque (*b*)

Most researchers have measured the extent or severity of delamination quantitatively using delamination factor. It is the ratio between the maximum delaminated and the nominal diameter. On the other hand, physical appearance analysis has also been used. In this case, scanning electron microscope or imaging software is used to check on the delaminated areas of the work piece. The finite element software uses color to indicate the extent of delamination on the part. The authors [3] used imaging software to compare the entry and exit delamination on experiments to that of FE results. Figure 14 shows the comparisons of experimental and finite element results of entry delamination.

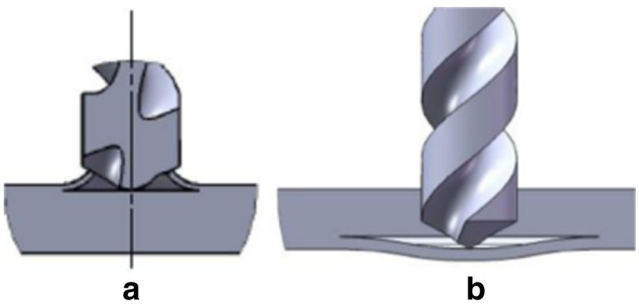

Fig. 12 Delamination mechanisms. **a** Peel-up. **b** Push-down [5]

From Fig. 15, the authors [38] compared experimental result of delamination they obtained by scanning the drilled work piece using scanning electron microscope (SEM) and that of FE model. The white spots depict complete delamination.

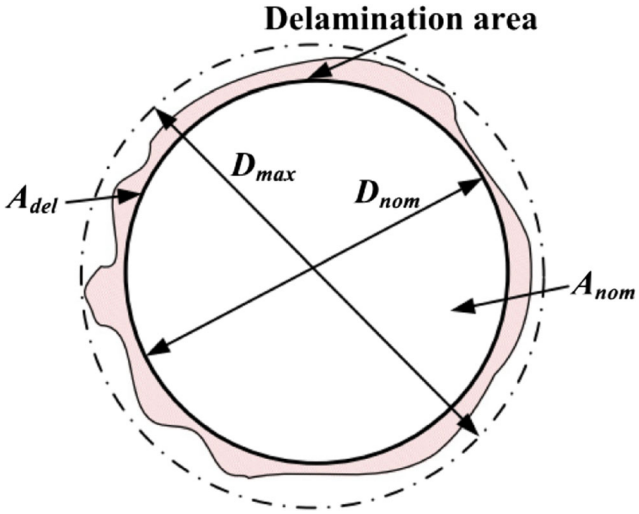

Fig. 13 Delamination factor measurement [8]

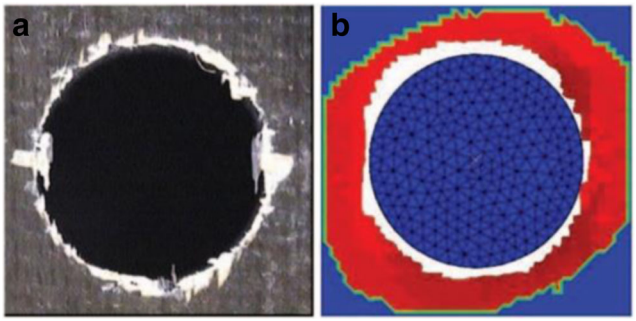

Fig. 15 Comparisons of entry delamination. **a** SEM. **b** FE model [38]

5 Conclusions

The remarkable mechanical and physical properties of CFRP composites are the main reason these materials are now being used in many applications led by aerospace industry. Drilling of these materials is a complex phenomenon resulting to different modes of damage that may compromise the performance of the structure or lead to catastrophic failures. It is for these reasons that many researchers and material enthusiasts are developing interests in understanding the damages caused by drilling to the CFRP using mainly experimental assessments and numerical simulations. Recently, 3D FE models that can predict intra-laminar and inter-laminar (delamination) damage on CFRP composite laminate induced by drilling have been developed using Abaqus/CAE software. There is no record in the published literature about review of this tremendous stride in research to guide new researchers. In this paper, a review of modeling 3D FE drilling simulation of CFRP has been done. The paper has focused on the recent work involving 3D simulation models of CFRP using Abaqus/CAE and whose results have been validated by experiments. From the available literature, the following observations can be made on the current state-of-the-art as far as FE modeling of CFRP drilling in Abaqus/CAE is concerned:

1. The most commonly used software has been Abaqus/CAE using the EXPLICIT solver.
2. Using solid elements for analysis (3D geometry) requires the use of Vectorized User Material (VUMAT) to implement damage criteria. The failure criterion available in the Abaqus/CAE software is only for shell elements (2D geometry).
3. A successful 3D model simulation will require the researcher to have additional knowledge about coding in Fortran language to write the VUMAT subroutine.
4. Hashin failure criterion proposed by Zvi Hashin in 1980 is the most employed to predict intra-laminar failure which includes fiber tension, matrix tension, fiber compression, and matrix compression. It is also included in the commercially available FE software Abaqus/CAE for shell elements.
5. Inter-laminar failure (delamination) has been modeled using two approaches namely cohesive elements and cohesive surfaces. The former involves the use of small thickness cohesive elements on the interfaces, whereas the latter is a surface interaction property.

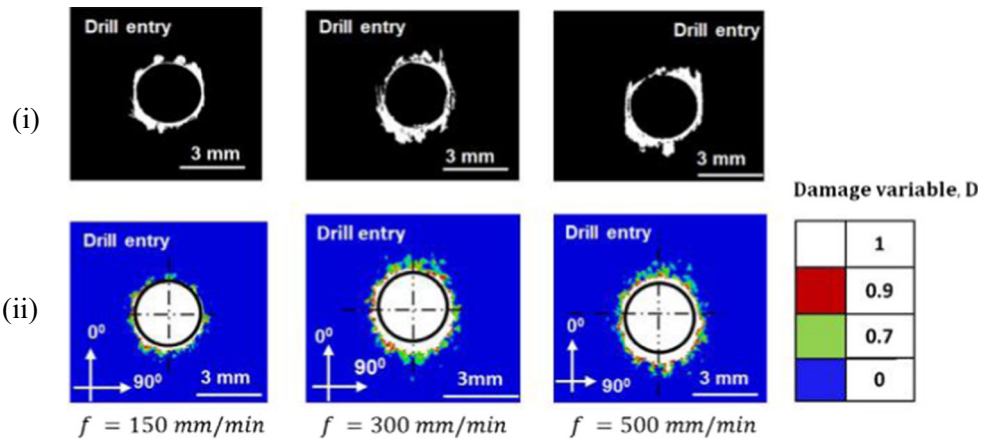

Fig. 14 Comparisons of **i** image processing (experimental) and **ii** FE model results of entry delamination [3]

6. A reference point on the drilling tool is created to record thrust forces involved in the process. It has been found to be responsible to delamination; hence, its monitoring is a priority.
7. The simulation run is a time-consuming process taking an average of about 15 days. It depends on the computing capabilities of the computer used, the number of elements, and the feed rate employed among other many factors.

Successful simulations have provided results having a high level of agreement with experimental results. The deviation between the results for most researchers has been less than 10% which is highly acceptable. The advance in the computing capabilities of computers continues to motivate the use of finite element modeling to study complex machining processes including drilling in detail. Various drilling parameters which can be difficult to achieve in experiments can easily be achieved in FE models. Therefore, the use of FE models is expected to increase in two-fold in a near future, and such a review paper is meant to provide basic guidance for new researchers in the field.

Compliance with ethical standards

Conflict of interest The authors declare that they have no conflict of interest.

References

1. Vicki P. McConnell. (2011) Materials today. [online]. http://www.materialstoday.com/composite-applications/features/past-is-prologue-for-composite-repair/
2. Bhatnagar N, Viswanath P, Singh I (2008) Drilling of unidirectional glass fiber reinforced plastics:Experimental and finite element study. Mater Des 29:546–553
3. Makhdum F, Roy A, Silberschmidt VV, Phadnis VA (2013) Drilling in carbon/epoxy composites: experimental investigations and finite element implementation. Compos Part A 47:41–51
4. de Moura MFSF, Marques AT, Dura LMP (2008) Numerical prediction of delamination onset in carbon/epoxy composites drilling. Eng Fract Mech 75:2767–2778
5. Teti R (2002) Machining of composite materials. CIRP Ann Manuf Technol 51(1):611–634
6. Shin YC, Chinmaya R (2012) Dandekar, "modeling of machining of composite materials: a review,". Int J Mach Tool Manu 57:102–121
7. Tang YJ, Cong WL, Liu DF (2012) A review of mechanical drilling for composite laminates. Compos Struct 94:1265–1279
8. Mkaddem A, Xu MEMJ (2016) Recent advances in drilling hybrid FRP/Ti composite: a state-of-the-art review. Compos Struct 135: 316–338
9. Tsao CC (2008) Experimental study of drilling composite materials with step-core drill. Mater Des 29:1740–1744
10. Herbert MA, Shetty D, Vijay GS, Shetty R, Shivamurthy Nagaraja B (2015) Experimental Investigation in Drilling of Carbon Fiber Reinforced Polymer Composite using HSS and Solid Carbide Drills. Int J Curr Eng Technol 5:1
11. Chiu YC, Tsao CC (2011) Evaluation of drilling parameters on thrust force in drilling carbon fiber reinforced plastic (CFRP) composite laminates using compound core-special drills. Int J Mach Tool Manu 51:740–744
12. Tsao CC (2008) Investigation into the effects of drilling parameters on delamination by various step-core drills. J Mater Process Technol 206:405–411
13. Kwon PY, Sturtevant C, Kim D(D-W), Wang JLX (2013) Tool wear of coated drills in drilling CFRP. J Manuf Process 15:127–135
14. Gerard Poulachona, Frederic Rossia, Rachid M'Saoubi Christophe Ramireza (2014) "Tool wear monitoring and hole surface quality during CFRP drilling." In 2nd CIRP 2nd CIRP Conference on Surface Integrity (CSI), pp. 163–168
15. Gehin D, Gutierrez ME, Girot F, Iliescu D (2010) Modeling and tool wear in drilling of CFRP. Int J Mach Tool Manu 50:204–213
16. Eneyew MRED (2014) Experimental study of surface quality and damage when drilling unidirectional CFRP composites. J Mater Res Technol 3(4):354–362
17. Aspinwall DK, Soo SL, Bradley S, Shyha IS (2009) Drill geometry and operating effects when cutting small diameter holes in CFRP. Int J Mach Tool Manu 49:1008–1014
18. Soo SL, Aspinwall D, Shyha SBI (2010) Effect of laminate configuration and feed rate on cutting performance when drilling holes in carbon fibre reinforced plastic composites. J Mater Process Technol 210:023–1034
19. Royer R, Merson E, Lockwood A, Ayvar-Soberanis S, Marshall MB, Merino-Pérez JL (2016) Influence of workpiece constituents and cutting speed on the cutting forces developed in the conventional drilling of CFRP composites. Compos Struct 140:621–629
20. S.L. Soo, D.K. Aspinwall, D. Pearson, W. Leahy, M.J. Li (2014) "Influence of lay-up configuration and feed rate on surface integrity when drilling carbon fibre reinforced plastic (CFRP) composites." In 2nd CIRP Conference on Surface Integrity (CSI), pp. 399–404
21. Tobias Pfeifroth Uwe Heisel (2012) "Influence of Point Angle on Drill Hole Quality and Machining Forces when Drilling CFRP," in 5th CIRP Conference on High Performance Cutting 2012, pp. 471–476
22. Habak M, Velasco R, Aboura Z, Khellil K, Turki PVY (2014) Experimental investigation of drilling damage and stitching effects on the mechanical behavior of carbon/epoxy composites. Int J Mach Tool Manu 87:61–72
23. A. Roy, V. V. Silberschmidt V. A. Phadnis (2012) "Finite element analysis of drilling in carbon fiber reinforced polymer composites." J Physics 382
24. López-Puente J, Santiuste C, Miguélez MH, Feito N (2014) Numerical prediction of delamination in CFRP drilling. Compos Struct 108:677–683
25. Isbilir EGO (2013) Numerical investigation of the effects of drill geometry on drilling induced delamination of carbon fiber reinforced composites. Compos Struct 105:126–133
26. Anish Roy, Vadim V. Silberschmidt Vaibhav A. Phadnis (2013) "A finite element model of ultrasonically assisted drilling in carbon/epoxy composites." In 14th CIRP Conference on Modeling of Machining Operations (CIRP CMMO), pp. 141–146
27. Phadnis VA, Roy A, Silberschmidt VV, Makhdum F (2014) Effect of ultrasonically-assisted drilling on carbon-fibre-reinforced plastics. J Sound Vib 333:5939–5952
28. Farrukh Makhdum, Anish Roy,Vadim V. Silberschmidt Vaibhav A. Phadnis (2012) "Experimental and numerical investigations in conventional and ultrasonically assisted drilling of CFRP laminate." In 5th CIRP Conference on High Performance Cutting 2012, pp. 472–476
29. Harland AR, Lucas T, Price D, Silberschmidt VV, Ullah H (2012) Finite-element modelling of bending of CFRP laminates: multiple delaminations. Comput Mater Sci 52:147–156
30. Sangwan SS, Bandhu MVD (2014) A Review of Drilling of Carbon Fiber Reinforced Plastic Composite Materials. Int J Curr Eng Technol 4:3

31. Stuart Barnes, Pipat Bhudwannachai Aishah Najiah Dahnel Drilling of carbon fibre composites: a review. Adv Mater Res, vol. 903, pp. 3–8, 2014.
32. Zhongwei G, Wesley C, Vo SG, Thuc (2012) Low impulse blast behaviour of fibre-metal laminates. Compos Struct 94(3):954–965
33. Zhongwei Guan and Wesley Cantwell Jin Zhou (2014) "Numerical modelling of perforation impact damage of fibre metal laminates." In ICCM2014, Cambridge
34. Swait T, Soutis C, Shi Y (2012) Modelling damage evolution in composite laminates subjected to low velocity impact. Compos Struct 94:2902–2913
35. Singh PMH (2015) Modeling damage induced plasticity for low velocity impact simulation of three dimensional fiber reinforced composite. Compos Struct 131:290–303
36. Iannucci L, Robinson P, Curtis PT, Raimondo L (2012) A progressive failure model for mesh-size-independent FE analysis of composite laminates subject to low-velocity impact damage. Compos Sci Technol 72:624–632
37. Hashin Z (1980) Failure criteria for unidirectional fiber composites. J Appl Mech 47(2):329–334
38. E. Ghassemieh O. Isbilir (2013) "Three-dimensional numerical modelling of drilling of carbon fiber-reinforced plastic composites." J Compos Mater
39. Sánchez-Sáez S, Barbero E, Santiuste C (2010) A comparison of progressive-failure criteria in the prediction of the dynamic bending failure of composite laminated beams. Compos Struct 92:2406–2414
40. Petrinic N, Ruiz C, Hallett SR, Hou JP (2000) Prediction of impact damage in composite plates. Compos Sci Technol 60(2):273–281
41. Zaera R, Navarro C, Lopez-Puente J (2008) Experimental and numerical analysis of normal and oblique ballistic impacts on thin carbon/epoxy woven laminates. Compos Part A 39:374–387
42. Schürmann H, Puck A (2002) Failure analysis of FRP laminates by means of physically based phenomenological models. Compos Sci Technol 62(12–13):1633–1662
43. Camanho PP, Costa J, Renart J, Turon A (2010) Accurate simulation of delamination growth under mixed-mode loading using cohesive elements: definition of interlaminar strengths and elastic stiffness. Compos Struct 92(8):1857–1864
44. Dassault systemes (2014) "Abaqus/CAE 6.14 user's guide"
45. Stephen Kirwa Melly, S.K. Kafi Ahmed, GongDong Wang (2016) "Finite element study into the effects of fiber orientations and stacking sequence on drilling induced delamination in CFRP/Al stack." Sci Eng Compos Mater
46. Ferret B, Lachaud F, Swider P, Piquet R (2000) Experimental analysis of drilling damage in thin carbon/epoxy plate using special drills. Compos A: Appl Sci Manuf 31(10):1107–1115
47. Tsao CC, Hocheng H (2005) The path towards delamination-free drilling of composite materials. J Mater Process Technol 167:251–264